(12)

NAVSWC TR 91-666

ELECTROSTATIC DISCHARGE INITIATION EXPERIMENTS USING PVDF PRESSURE TRANSDUCERS

BY RICHARD J. LEE, DOUGLAS G. TASKER, and MAI-TRAM CONG

RESEARCH AND TECHNOLOGY DEPARTMENT

DECEMBER 1991

NAVAL SURFACE WARFARE CENTER

Dahlgren, Virginia 22448-5000 • Silver Spring, Maryland 20903-5000

NAVSWC TR 91-666

ELECTROSTATIC DISCHARGE INITIATION EXPERIMENTS USING PVDF PRESSURE TRANSDUCERS

BY RICHARD J. LEE, DOUGLAS G. TASKER, and MAI-TRAM CONG

RESEARCH AND TECHNOLOGY DEPARTMENT

DECEMBER 1991

NAVAL SURFACE WARFARE CENTER

Dahlgren, Virginia 22448-5000 • Silver Spring, Maryland 20903-5000

FOREWORD

Naval munitions, especially those contained in insulating cases, are at risk due to electrostatic discharge (ESD). Electrical energy can be stored on such cases through electrostatic charging by normal handling or thermal cycling. The energy deposited in the energetic material in a single event comes from a small fraction of the case surface. Until recently the problem of ESD ignition has been of concern with large rocket motors because of their size, i.e., their ability to store more energy across their surface. However, the realization that a small area of the case can store a sufficient energy to ignite energetic materials, e.g., less than 10 mJ, places small devices in jeopardy as well.

Existing Navy test procedures do not adequately determine the risks associated with ESD from insulating cases. Present certification tests were designed to rank the relative safety of energetic materials with respect to discharges from human bodies. The electrical discharge in encased energetic materials is an entirely different situation; the electrostatic energy is transferred more efficiently since the intimate contact between the case and the energetic material minimizes any dissipative and inductive elements in the discharge path. A number of different factors, inherent to encased energetic materials, sensitize the material to ESD ignition, e.g., casting stresses, containment, and the inclusion of air. None of these factors are addressed in existing Navy test procedures.

Experiments like those reported here are crucial to determining how the electrostatic energy stored on insulating cases can cause ignition in energetic materials. This understanding is necessary to define the relative hazard and to establish effective techniques to reduce the hazard.

We thank B. Hammant of Ministry of Defense, U.K., for his helpful comments on this work. We are indebted to R. Hay for his fine experimental work.

Approved by:

WILLIAM H. BOHLI, Acting Head
Energetic Materials Division

ABSTRACT

Electrical discharge experiments were performed on an aluminized explosive, PBXW-115. Simultaneous observations of polyvinylidene difluoride (PVDF) pressure sensor signals, and the deposition of electrical power were recorded. These data were compared to those from similar experiments performed on aluminized inert material and in air gaps. Distinct pressure differentials were observed during the discharge phase following a delay after dielectric breakdown. The signals from the pressure sensors are comparable for each case, i.e., the unreacted PBXW-115, the ignited PBXW-115, the inert solids, and the air gaps. It is believed that sustained ignition occurred in the explosive after the electrical energy deposition following a long incubation period (< 10 ms). Containment of the building reaction, and the presence of air adjacent to the explosive sample were found to have a significant effect on the ignition sensitivity. The results are discussed within the context of a preliminary model of electrostatic initiation.

CONTENTS

Chapter		Page
1	INTRODUCTION	1-1
	TWO PHASE IGNITION MODEL	1-1
	SENSITIZING FACTORS	1-2
2	EXPERIMENTAL	2-1
	TEST SAMPLES	2-1
	TEST CELL	2-3
	DIAGNOSTICS	2-6
3	RESULTS	3-1
	SUSTAINED REACTION CONDITIONS	3-1
	PVDF PRESSURE SENSOR DATA	3-4
	DELAYED REACTION	3-5
	ENERGY DEPOSITION	3-5
4	DISCUSSION	4-1
	PVDF SENSOR DIAGNOSTICS	4-1
	SUSTAINED REACTION CONDITIONS	4-3
	FUTURE WORK	4-3
5	CONCLUSIONS	5-1
	REFERENCES	6-1

Appendix		Page
A	TABULATED RESULTS	A-1

ILLUSTRATIONS

Figure		Page
2-1	NOMINAL TEST CELL ARRANGEMENT	2-4
2-2	COMPARISON OF ALTERNATE TEST CELL ARRANGEMENTS	2-5
2-3	RELATIVE LOCATION OF PRESSURE SENSORS, EXPLODED	2-7
3-1	TEST CELL AFTER IGNITION EXPERIMENT	3-2
3-2	TEST SAMPLE AFTER FAILED IGNITION EXPERIMENT	3-2
3-3	TYPICAL VOLTAGE, CURRENT AND PRESSURE SIGNAL PROFILES	3-3

TABLES

Table		Page
2-1	CONSTITUENT DATA FOR PBXW-115	2-2
2-2	CONSTITUENT DATA FOR MICOM INERT SAMPLES	2-2
2-3	CONSTITUENT DATA FOR ALUMINUM WAX SAMPLES	2-2
A-1	EXPERIMENTAL DESCRIPTION FOR INERT SAMPLES	A-1
A-2	DESCRIPTION AND IGNITION RESULTS FOR PBXW-115	A-2
A-3	PVDF PRESSURE SENSOR DATA	A-3

CHAPTER 1

INTRODUCTION

Energetic materials contained in composite casings have been recognized as being prone to ignition due to electrostatic discharge (ESD).[1,2] The propellant or explosive contained within the casing is subject to ignition via the rapid discharge of electrostatic energy from the case. The energy is stored on the case through electrostatic charging as a result of relative motion and subsequent separation of system materials (triboelectrification). The inherent danger is that substantial charges can be generated through normal handling of the system.

The electrostatic energy per unit area stored on a case from triboelectrification is estimated to be on the order of 100 mJ/m^2.[3] It is useful to think of the energy in these terms since it is expected that the charge contained on a small section of the surface will be depleted in a single discharge event. Hence, a single discharge may only dissipate energies in the 10 mJ range. Until recently, the problem of ESD ignition has been concerned with large rocket motors because of their size, i.e., their ability to store more energy across their surface. However, the realization that a small area of the case, $\leq 1/3$ m in diameter, can store a sufficient energy to ignite energetic materials places small devices in jeopardy as well.

It is important to understand how such small energies can cause ignition in energetic materials so that the relative hazard associated with ESD can be accurately defined. This understanding is necessary to establish effective techniques to reduce the hazards associated with ESD ignition.

TWO-PHASE IGNITION MODEL

A model has been proposed which describes a two-phase ignition process for ESD.[4,5] In this model it is hypothesized that adiabatic heating of the arc channel leads to reaction of the material in the arc channel. The energy released from the chemical reaction in the channel serves to drive the second phase of ignition in the unreacted material beyond the arc channel. It is surmised that there is a critical volume for the arc channel, above which the secondary reaction will be self-sustaining and will accelerate. The critical volume is based on a sufficient

release of energy from the initial reaction in order for this reaction to continue beyond the arc channel.

Note that the hypothesis of two distinct phases of ignition suggests that there should be two distinct pressure profiles; the detection of these profiles would support the model.

SENSITIZING FACTORS

The available energy from a charged case is several orders of magnitude smaller than those energies used to certify energetic materials. Hence, there must be certain sensitizing factors which serve to decrease the electrical energy required for ignition. It has been suggested that high electrical powers, not necessarily large energies, are crucial for ESD ignition.[3] The power input determines the initial release of chemical energy from the arc channel. The ambient gas pressure is another sensitizing factor. Hodges[6] reported that the threshold ignition energy for a PBAN composite aluminized propellant was reduced from 3.7 J to 90 mJ when subjected to a static nitrogen pressure of 2.0 MPa (300 psig). The study, discussed in this report, demonstrated that containment of the reaction, and the inclusion of air, significantly affect the ESD ignition sensitivity.

CHAPTER 2

EXPERIMENTAL

Polyvinylidene difluoride (PVDF) pressure sensors[7,8] were used to detect pressure differentials in an aluminized explosive, PBXW-115, during electrical discharge experiments. The data were compared to those from several inert samples: aluminized wax, an aluminized propellant stimulant obtained from the Missile Command (MICOM) at Redstone Arsenal, and air gaps. Electrical energies were deposited in the samples from a 50 μF capacitance charged to 5 kV. This circuit provided electrical power up to 10 MW and deposition energies exceeding 150 J.

The intent of these experiments was to deposit a high power electrical discharge in explosive samples, and measure the time to the onset of reaction. This technique would provide a measure of the electrical energy necessary for ignition in a single experiment.

TEST SAMPLES

The explosive and solid inert test samples were cylindrical disks 44.45 mm diameter by 6.35 mm thick. The constituents for each solid test material are provided in Tables 2-1 through 2-3. The aluminized wax material was a rudimentary first attempt at simulating the PBXW-115. It proved difficult to maintain a uniform concentration of aluminum along the length of the sample. However, the crucial requirement was to provide enough aluminum to facilitate dielectric breakdown rather than to try to simulate the precise electrical properties of PBXW-115.

The MICOM inert was not an exact replica of PBXW-115 either, but it was available and the material morphology was better controlled. Unfortunately, the dielectric breakdown strength of the MICOM samples ($\approx$ 1.5 MV/mm) exceeded the experimental operating voltage. The 5 kV power supply only produced an electric field of 0.8 MV/mm across the 6.35 mm sample. This problem was circumvented by forcing dielectric breakdown in the sample prior to the discharge experiment.

The air gaps were produced by using a 3.18 mm diameter hole in a Teflon spacer, 6.35 mm thick. Dielectric breakdown was assisted by scribing a pencil mark along the internal wall of the hole.

TABLE 2-1. CONSTITUENT DATA FOR PBXW-115

Ammonium Perchlorate	43%	Aluminum	25%
RDX	20%	HTPB Binder	12%

TABLE 2-2. CONSTITUENT DATA FOR MICOM INERT SAMPLES

Sodium Chloride (200 μ)	51%	Aluminum	19%
Ammonium Sulfate (20 μ)	17%	HTPB Binder	12%
IPDI (curative)	0.8%	HX752 (catalyst)	0.5%

TABLE 2-3. CONSTITUENT DATA FOR ALUMINUM WAX SAMPLES

Paraffin Wax	75%	Aluminum*	25%

* Concentration of aluminum in wax samples was not uniform due to the aluminum settling towards the bottom during the setting process.

TEST CELL

Each sample was fitted into a plastic test cell, shown in Figure 2-1. The nominal test cell consisted of two brass electrodes (a cylindrical disk and a bar), a polymethyl methacrylate (PMMA) containment cylinder and two Teflon end caps (the retaining ring and the base cap). Four steel retaining bolts (not shown in the figure) held the test cell together.

The high voltage electrode was a 19 mm diameter brass rod which was connected to a brass disk (47.63 mm diameter) used for electrical connections. A 6.35 mm thick Teflon spacer around the electrode displaced the air adjacent to the test sample. In some experiments the effect of the presence of air was determined by either removing the Teflon spacer or using a similar high voltage electrode on the end of a brass threaded rod.

Note that various test cell arrangements, representing a progression in development to the final test cell shown in Figure 2-1, were used in this study. The five different combinations of electrode arrangement are shown in Figure 2-2. Tables A-1 and A-2, in Appendix A, indicate which electrode arrangement was used for each experiment.

In all but two cases, the *low voltage* electrode was a 15.88 mm wide, 3.18 mm thick bar which was fitted into a groove in the bottom end cap. The groove allowed the electrode face and the bottom end cap to fit flush against the sample. This electrode was covered by a 60 μm thick insulating mask which had a circular opening (4.6 mm diameter) through which the electrode made contact with the explosive. This configuration provided control over the time to dielectric breakdown, and ensured that the arc channel would be centrally located with respect to the low voltage electrode.

Experiment 115-4 was one of the exceptions concerning the low voltage electrode. A cylindrical disk electrode was used *in lieu* of the brass bar. This arrangement, shown in Figure 2-2(a), is the original test cell used in earlier studies between 1988 and 1989. Experiment 115-6 was the other exception which used a 12.7 mm wide copper foil *in lieu* of the brass bar.

The degree of containment was determined by the integrity of the containment cylinder. Four variations of the cylinder configuration were used: a thin-walled tube (1.59 mm wall thickness); a thick-walled tube (9.53 mm wall thickness); the thick-walled tube reinforced with four layers of cloth tape; and the thin-walled tube reinforced with cloth tape and a metal hose clamp.

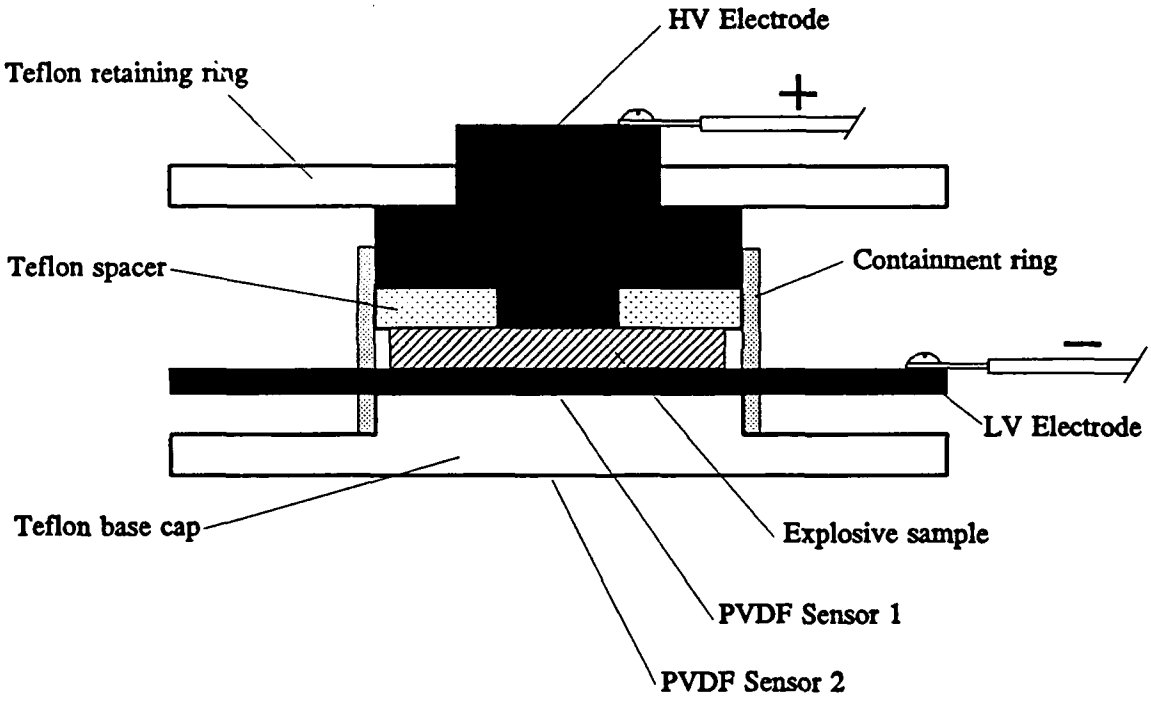

FIGURE 2-1. NOMINAL TEST CELL ARRANGEMENT

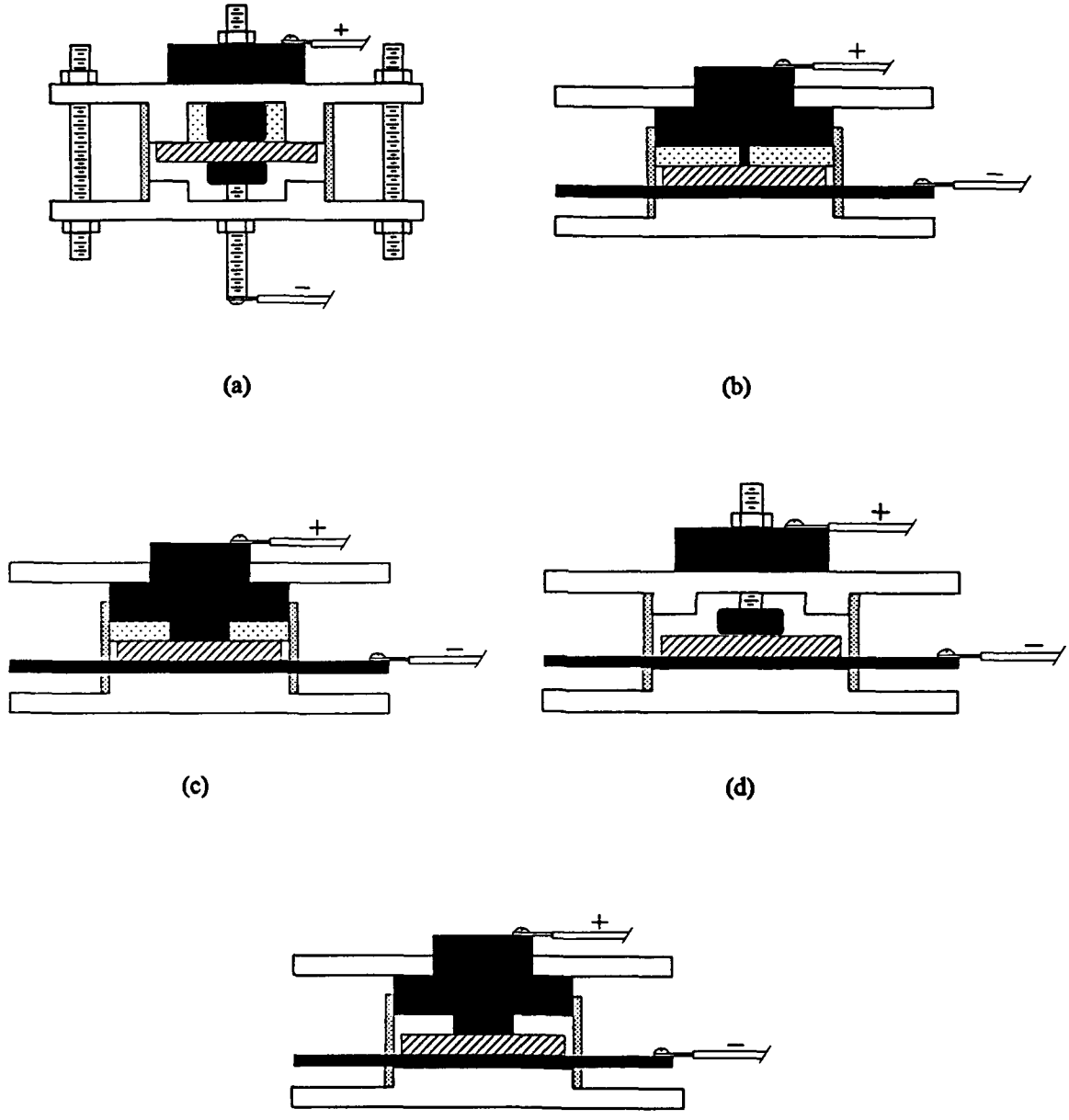

FIGURE 2-2. COMPARISON OF ALTERNATE TEST CELL ARRANGEMENTS

DIAGNOSTICS

A copper sulphate voltage probe[9] was connected directly across the two electrodes to minimize inductive errors, insuring an accurate measure of the voltage across the test sample. A Pearson current transformer measured the total current in the circuit. A Rogowski coil[7] placed around the high voltage leads measured the rate of current change, dI/dt, through the sample.

Two PVDF pressure sensors, 12.5 mm wide by 30 mm long, were used to obtain timing markers, i.e., to detect when any pressure differential occurred in the sample during the electrical discharge. Note that the initial intent behind using these sensors did not require an accurate measurement of the pressure. The PVDF sensors used in this study were not calibrated, hence any accurate measurement of pressure was not possible.

The large sensor area was employed so that the arc channel would be directly over the sensor. There is a nonlinear relationship between pressure and the charge density, i.e., charge per unit area, developed in the sensor material. Hence, the area of the sensor affected by any disturbance must be known to obtain an accurate measurement of the pressure. The data from these experiments could not have been related to pressure since the affected sensor area could not be defined. Furthermore, the divergence of the shock profile coming from the arc channel would introduce errors in the measurement since the calibration data are based on uniaxial stress profiles.

Figure 2-3 shows the relative location of each pressure sensor with respect to the bottom section of the test cell. The first pressure sensor was placed under the cathode, and the second sensor was located below the first gauge, on the back side of the test cell. The 6.36 mm thick Teflon retaining cap separated the two gauges. Another Teflon cap, with a brass bar inserted in the groove, was normally used as a backing plate for the second gauge. Four later experiments used a 6.36 mm PMMA plate for this function to minimize any flexing of the base cap.

The pressure sensors were used in either the so-called "charge" or "current" modes which normally yield pressure data, P, or dP/dt, respectively. The first sensor was operated in either the "charge" mode or the "current" mode. The second sensor always was operated in the "current" mode, and was used to verify the integrity of the signal obtained by the first gauge. This method of verification proved worthwhile since the first sensor occasionally experienced signal distortions due to noise pickup from the low voltage electrode.

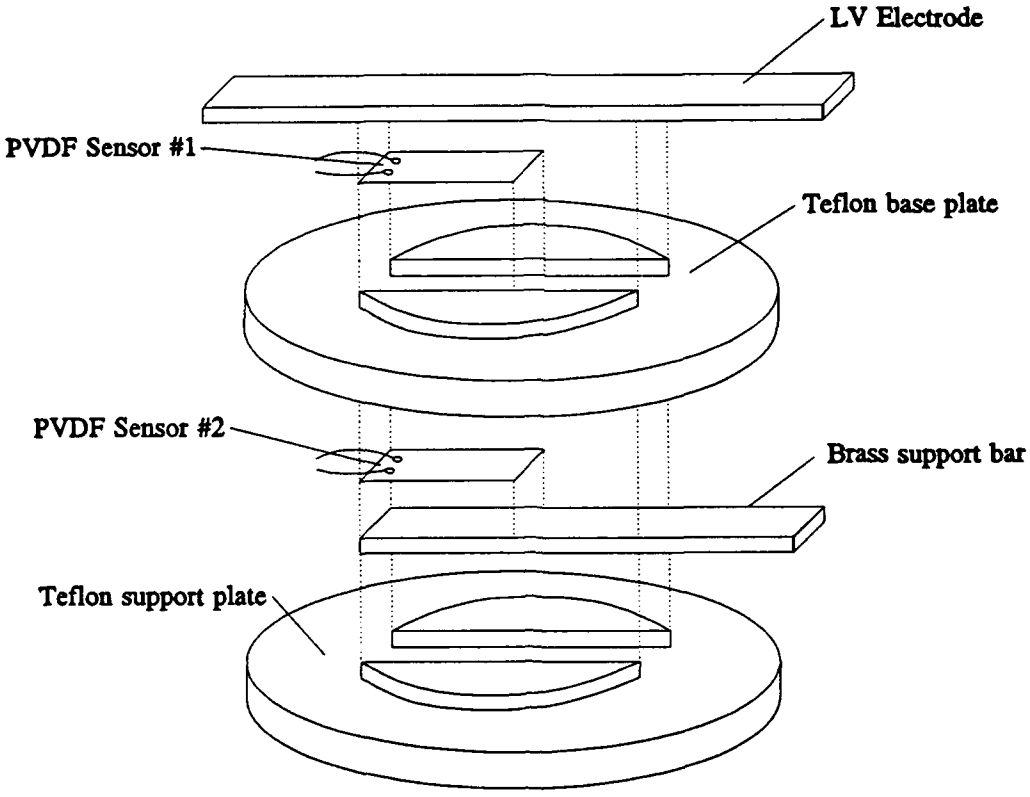

FIGURE 2-3. RELATIVE LOCATION OF PRESSURE SENSORS, EXPLODED

CHAPTER 3

RESULTS

SUSTAINED REACTION CONDITIONS

Sustained reaction was observed, i.e., the explosive was consumed, when two conditions were met: (1) the containment cylinder was not ruptured, and (2) air was present in the test cell. If either one of the above criteria were not met then a single hole was left in the sample, with radial cracks emanating from it, as shown in Figure 3-1. In some cases the sample was shattered into several pieces.

The need for a stronger confinement cylinder became obvious during the first attempts to exclude all air along both faces of the test sample. The thin cylinder provided adequate containment only when air was present in the test cell. These cylinders were typically deformed as a result of any reaction but were recovered intact, as shown in Figure 3-2. To maintain the integrity of the test cell when the air was excluded, it was necessary to reinforce the cylinders. This observation suggests that when air is excluded the pressure in the test cell is significantly higher.

It is interesting to note experiments 115-11 and 115-12 concerning the need for containment. The containment rings for these two experiments were designed to maintain containment. However, the containment was lost through an opening between the slits at the base of the containment ring and the bar electrode. These slits were originally cut so that the containment ring would fit tightly over the bar electrode. However, repeated polishing reduced the size of the electrode thereby allowing gases to vent between the electrode and the Teflon. Care was taken in subsequent experiments to maintain a close fit between the containment ring and the bar electrode.

Particular information concerning each experiment (electrode configuration, air inclusion and whether containment was maintained) is listed with the ignition results in Appendix A (Table A-2). The same information concerning the arrangements for the inert experiments is given in Table A-1.

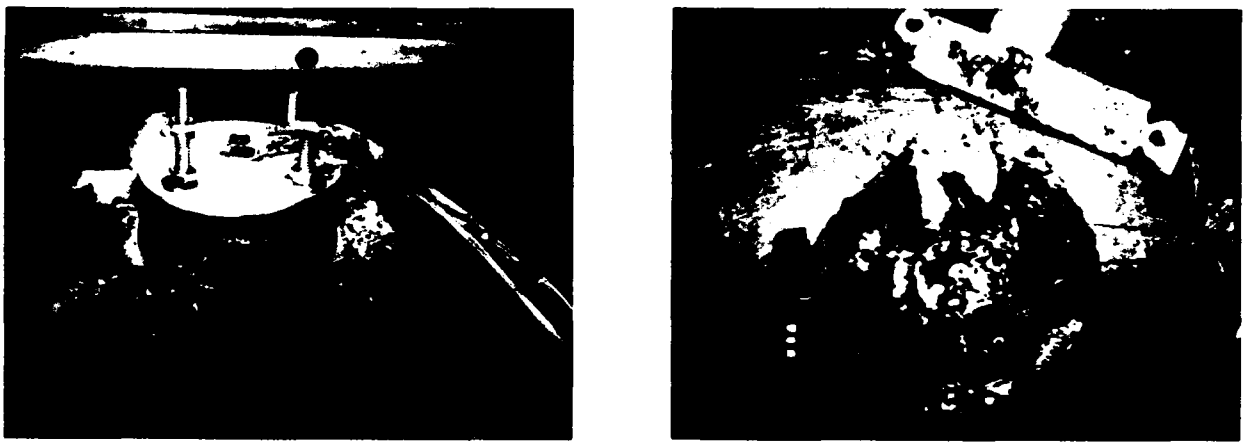

FIGURE 3-1. TEST CELL AFTER IGNITION EXPERIMENT

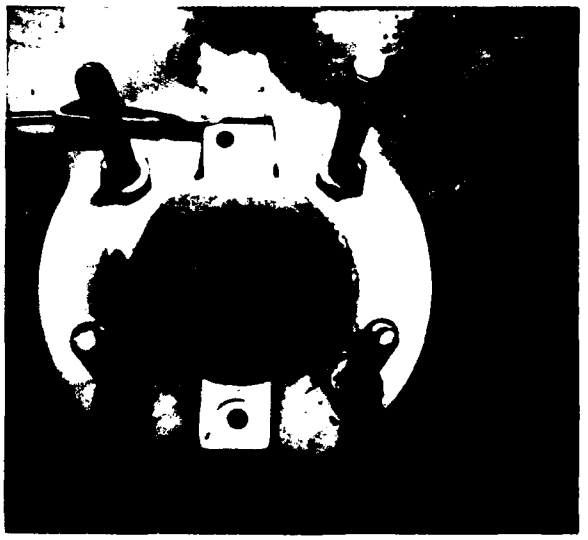

FIGURE 3-2. TEST SAMPLE AFTER FAILED IGNITION EXPERIMENT

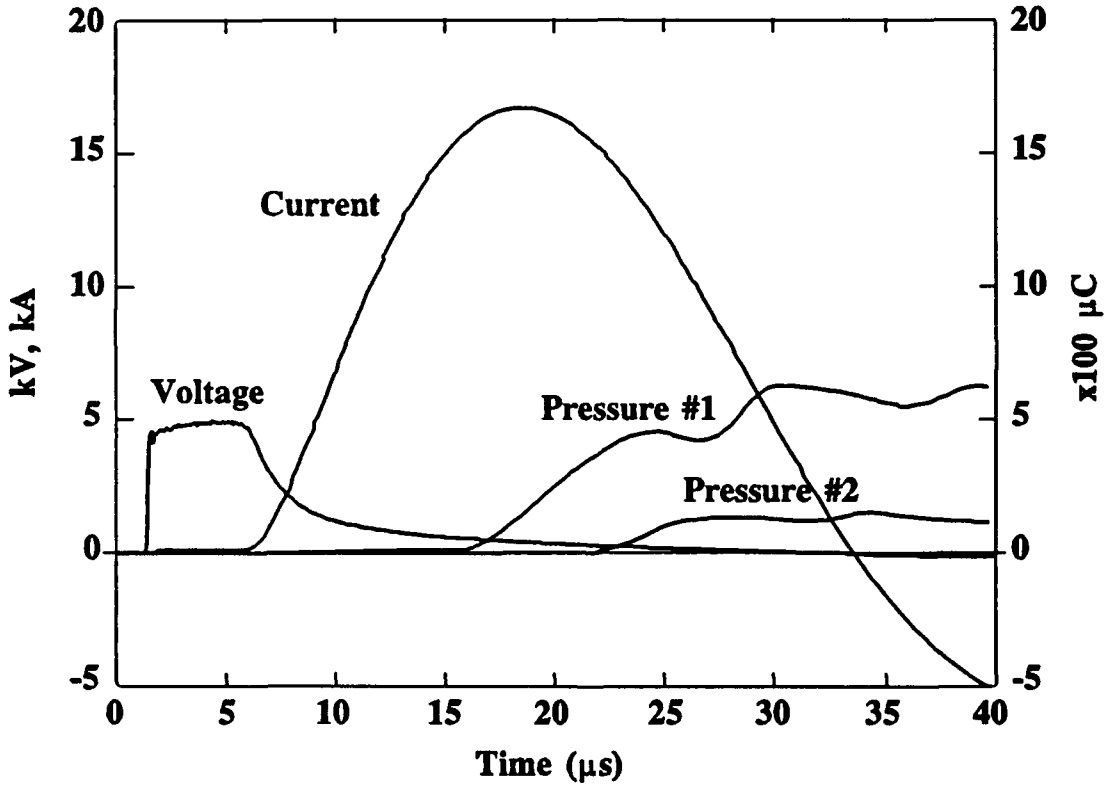

FIGURE 3-3. TYPICAL VOLTAGE, CURRENT AND PRESSURE SIGNAL PROFILES

PVDF PRESSURE SENSOR DATA

The current, voltage and both pressure signals for one experiment are plotted on the same graph in Figure 3-3 to provide an instructional view of when the pressure signals were recorded during an experiment.

The pressure sensor data for all the materials studied (PBXW-115, aluminized wax, the MICOM inert and the air gaps) are comparable. This comparison also holds for those samples that were consumed. A sharp rise in the pressure was observed between 1.8 and 33.7 μs after dielectric breakdown. The second pressure sensor detected the signal after a delay which varied between 3.4 and 19.4 μs after the first pressure sensor. Note that 3.5 μs is consistent with an average transit velocity comparable to the sound speed (1.84 mm/μs).

The pressure sensor records are related to the charge, and not the pressure, because the affected area of the pressure sensor was not defined. The PVDF sensor signals reached peak values between 94 nC and in excess of 700 nC. It is interesting that one of the largest signals (627 nC) was recorded for an explosive sample (115-10) which did not ignite. The mean signal peaks for the two sensors are 193 nC and 102 nC, respectively.

The containment ring for one of the MICOM inert samples (NRT-3) was left off to observe the effect on the pressure signal magnitudes. The first PVDF signal exceeded 700 nC and the second signal peaked at 67 nC.

The backing plate for the second pressure sensor was left off in another MICOM inert experiment (NRT-4) to determine if the signals were due to lateral strain in the PVDF sensor. Any lateral strain effects could be attributed to a flexing or bending of the bar electrode and the Teflon base plate, which were in contact with the pressure sensors. The second pressure sensor, having been open to a free surface, would not have registered any significant compressional forces. The second sensor in this experiment registered half of the nominal signal peak observed in experiments which used the backing plate. However, the second gauge in two experiments (NRT-1 and NRT-3) which did use a backing plate registered signals of similar magnitudes.

The last four experiments performed in this study (explosive samples 115-13 through 115-16) used a 6.35 mm thick PMMA backing plate behind the bottom end cap. This plate was employed to minimize bending of the electrode and, hence, stretching of the pressure sensor. The second gauge was not used in these experiments. The signal magnitudes were comparable to those in previous experiments.

The tabulated PVDF pressure sensor data are given in Appendix A (Table A-3) for selected experiments on PBXW-115 and inert samples. The sensor data for those experiments not represented in this table were either corrupted or not recorded due to signal pick up or other experimental difficulties.

DELAYED REACTION

The observation time for the PVDF signals in experiments 115-13 through 16 was extended to 20 ms. These records show the PVDF signals lasting well past the duration of the discharge. The electrical discharge was typically over after 80 μs while the PVDF signal could continue up to 8 ms. It is interesting to note that for experiment 115-13, an experiment in which ignition occurred, a second PVDF signal rise was observed 17 ms after dielectric breakdown. These long signals are consistent with strain effects in the test cells.

ENERGY DEPOSITION

The electrical energy deposited prior to breakdown varied between 1.8 and 3.9 J. The energy deposited between the dielectric breakdown time and the onset of the PVDF sensor signal varied between 5 and 150 J.

CHAPTER 4

DISCUSSION

PVDF SENSOR DIAGNOSTICS

The intent of this study was to deposit a high power electrical discharge in explosive samples, and measure the time to the onset of reaction in two distinct phases of ignition. Hence the PVDF sensors were only meant to detect pressure differentials which were to be used as timing markers. In our ignition model it is hypothesized that the highly localized electrical energy causes reaction in the material associated with the arc channel. It is assumed that the electrical energy is small compared to the heat of reaction, and hence has little effect on the secondary reaction beyond the channel. So, it should be possible to determine the energy to ignition in a single experiment if the initial reaction in the channel can be detected. A second pressure rise, marking the onset of reaction beyond the arc channel, is expected to follow some time after the initial reaction in the channel.

The PVDF sensor signals and the physical damage to the test cell observed in these experiments suggested that a slowly building pressure was developed in the sample. Since similar signals were observed in inert samples and air gaps, this pressure was not likely due to any building reaction in the material beyond the arc channel. It is more likely that the pressure was the result of some process restricted to the arc channel.

Mild shocks are typical for any arc discharge, but the pressure is expected to be on the order of 1.0 MPa.[10] Furthermore, any disturbance of this nature should be detectable at the same time the arc channel is formed, i.e., immediately following dielectric breakdown. Hence, it is not likely that the PVDF sensors detected a shock coming from the arc channel. The inconsistencies in the PVDF data which support this conclusion are as follows:

a) The delays between dielectric breakdown and the PVDF signals were in excess of 1 μs, and varied between 1.8 and 33.7 μs.

b) The delays between the two PVDF signals did not always correspond to the sound speed in the Teflon end cap. This delay varied between 3.4 and 19.4 μs.

It is plausible that the PVDF signals were indirectly caused by a shock wave from the arc channel, i.e, from lateral strain due to a bending of the electrode and the Teflon end cap. This bending would be consistent with the above observations. The signal magnitudes and the delays would depend on the mechanical motion of the electrode and the Teflon end cap following the shock wave. It is likely that this motion would not be the same for each experiment.

The large PVDF signal obtained in the experiment, where the containment ring was left off (NRT-3), provided the first clue that the PVDF signals could be the result of lateral strain. It is likely that the absence of the confinement ring allowed the test cell to flex more than usual, hence increasing the lateral strain in the sensor. The brass bars, having been bent in each experiment, corroborated this thinking. The conclusive evidence that at least a considerable fraction of the PVDF signals were due to lateral strain, was obtained in experiment NRT-4. The backing plate for the second pressure sensor was left off in this experiment. The second pressure sensor having been open to a free surface could not have registered any compressional forces. The second sensor in this experiment registered half of the nominal signal peak observed in experiments which used the backing plate. However, the second gauge in two experiments (NRT-1 and NRT-3) which did use a backing plate registered signals of a similar magnitude. Those experiments which used a PMMA backing plate, to provide more rigidity behind the electrode, can be overlooked in this argument since it is difficult to determine if the electrodes flexed or not. Given the wide variability in signal magnitudes between experiments, and the above observations concerning the signal delays, it is likely that the PVDF signal observed in each experiment was due largely to lateral strain.

Although the above observation casts aspersions on the pressure data, it supports the idea that significant pressures were being developed in the test sample prior to any reaction. The reason that these pressures were not directly detected was due to the large area of the sensor (375 mm^2). Any signal produced by a shock wave from the arc channel would affect an area with a diameter comparable to that of the arc channel, e.g., $\leq$ 1 mm. Conversely, the entire gauge would be affected from lateral strain effects. Since a large area sensor was used, it is possible that the voltage signal from lateral strain would be several orders of magnitude larger than that from a shock coming from the arc channel.

Despite the above argument concerning lateral strain, it is still possible to use PVDF pressure sensors to measure the ignition energy. The results of this study only suggest that more care must be taken in order to detect the pressure signals of interest. The lateral strain problem can be eliminated by using a more rigid test arrangement. Smaller PVDF sensors can be used to minimize the error associated with defining the affected area and divergent shock fronts.

SUSTAINED REACTION CONDITIONS

The results of the experiments conducted on the PBXW-115 demonstrate that containment and the inclusion of air are significant sensitizing factors for ESD ignition.

Containment

The need for containment to achieve a sustained reaction suggests that a slow building reaction occurs. What is not clear is when the onset of reaction occurs. For one of the experiments in which ignition occurred, 115-13, a second PVDF signal rise was observed 17 ms after dielectric breakdown. This second PVDF signal occurred well after the initial PVDF signal had decayed. It is possible that this late pressure rise was due to the onset of ignition in the explosive beyond the arc channel. This observation suggests that sustained ignition may occur in the explosive after the electrical energy deposition following a long incubation period (>10 ms).

Air Inclusion

It is not clear why air was also necessary to achieve a sustained reaction in these tests. It is possible that the air participates in the reaction, thereby increasing the perceived sensitivity to ignition. An earlier explanation based on a modification of the arc channel dynamics was discarded. It was believed that the sensitivity increased due to a focusing of the arc channel via electric field enhancement at the electrode-air-explosive triple junction. This argument was disproved after a sample was ignited in an experiment where the arc channel was centrally located with respect to the electrodes.

FUTURE WORK

Future studies will determine how the electrical power, pressure, containment and inclusion of air affect the ESD ignition sensitivity. Improvements to the pressure diagnostics will provide the detection of the reaction in the arc channel,

and the subsequent reaction beyond the channel. Photographic observations will confirm the time and degree of reaction.

CHAPTER 5

CONCLUSIONS

The PVDF pressure sensors did not directly detect any pressure development because of lateral strain effects. Consequently, any initial reaction in the arc channel associated with a first phase of ignition has yet to be confirmed. The onset of reaction, for the second phase of ignition beyond the arc channel, was not detected as well. The PVDF signals observed, and the physical damage to the test cells during these experiments, suggest that a significant pressure was developed in the sample. It is believed that both the onset of reaction in the arc channel and in the material beyond the arc channel can be detected with more carefully designed PVDF pressure gauges.

Containment of the reaction and the presence of air adjacent to the explosive sample were noted as two synergistic factors necessary for a sustained reaction in electrical discharge experiments. The need for containment to achieve a sustained reaction suggests that a slow building reaction occurs. The apparent enhancement in the reaction due to the inclusion of air is not yet understood. However, this effect suggests that air voids existing in encased explosives or propellants may sensitize them to ESD ignition.

REFERENCES

1. Technical Investigation of 11 January 1985 Pershing II Motor Fire, U.S. Army Missile Command, Redstone Arsenal, AL, Technical Report RK-85-9, Jun 1985.

2. M592 Mishap Report, 29 December 1987, TRW-25762, Thiokol Inc., Strategic Operations, Oct 1989.

3. R. J. Lee and D. G. Tasker, "Electrostatic Initiation Within Cased, Energetic Materials," 1991 JANNAF Propulsion Systems Hazards Subcommittee Meeting, Albuquerque, NM, Mar 1991.

4. R. J. Lee, D. G. Tasker, J. W. Forbes, B. C. Beard and J. Sharma, "Shock Ignition of an Explosive Due to Electrostatic Discharge (ESD)," Shock Waves in Condensed Matter, Albuquerque, NM, Aug 1989.

5. R. J. Lee, D. G. Tasker and J. W. Forbes, "Shock Ignition of an Explosive Due to Electrostatic Discharge (ESD)," 1990 JANNAF Propulsion Systems Hazards Subcommittee Meeting, Laurel, MD, Apr 1990.

6. R. V. Hodges and L. E. McCoy, "Ignition of Solid Propellant by Internal Electrical Discharge," JANNAF Propulsion Systems Hazards Subcommittee Meeting, Albuquerque NM, Mar 1991.

7. R.A. Graham, F. Bauer, L.M. Lee and R.P. Reed, "Standardized Bauer Piezoelectric Polymer Shock Gauge," Shock Wave Compression of Condensed Matter (proceedings of the Duvall Symposium, Washington State University, 1988), pp. 47-50.

8. L.M. Moore, R.A. Graham, R.P. Reed, M.U. Anderson, L.M. Lee, F.M. Horine, F. Bauer and T.W. Warren, "PVDF Gauge Applications," PVDF Shock Sensor Workshop Proceedings, Sandia National Laboratories, Albuquerque, NM, Dec 1990, pp. 145-178.

9. R. J. Lee and D. G. Tasker, "The Acquisition of Definitive ESD Sensitivity Data and a New Test Method," 1987 JANNAF Propulsion Systems Hazards Subcommittee Meeting, Huntsville, AL, Mar 1987.

10. T. Facklam, "Chemical Decomposition and Pressure Rise in Gaseous and Liquid $C_2Cl_3F_3$ under Internal Arc Stress," IEEE Transactions on Electrical Insulation, Vol. EI-20, No. 2, Apr 1985.

APPENDIX A

TABULATED RESULTS

TABLE A-1. EXPERIMENTAL DESCRIPTION FOR INERT SAMPLES

SAMPLE NUMBER	ELECTRODE ARRANGEMENT (LV TO HV)*	AIR INCLUSION	CONTAINMENT MAINTAINED	IGNITION
ALW-1	POINT TO BAR (a)	NO	NO	NO
ALW-2	POINT TO BAR (a)	NO	NO	NO
NRT-1	POINT TO BAR (a)	NO	NO	NO
NRT-2	DISK TO BAR (d)	YES	NO	NO
NRT-3	DISK TO BAR (d)	NO	YES	NO
NRT-4	DISK TO BAR (d)	NO	YES	NO
AIR-7	DISK TO BAR (d)	YES	YES	YES
AIR-8	DISK TO BAR (d)	YES	YES	YES

* High voltage (HV) electrode to low voltage (LV) electrode arrangement used for each experiment. The letter in parentheses indicates the particular electrode arrangement shown in Figure 2-2.

Key:
ALW - aluminized wax samples.
NRT - inert samples from MICOM.
AIR - air gap experiments.

TABLE A-2. DESCRIPTION AND IGNITION RESULTS FOR PBXW-115

SAMPLE NUMBER	ELECTRODE ARRANGEMENT (LV TO HV)*	AIR INCLUSION	CONTAINMENT MAINTAINED	IGNITION
115-1	POINT TO BAR (b)	NO	NO	NO
115-2	DISK TO BAR (c)	NO	NO	NO
115-3	DISK TO BAR (c)	NO	NO	NO
115-4	DISK TO DISK (a)	YES	NO	NO
115-5	DISK TO BAR (c)	NO	YES	NO
115-6	DISK TO FOIL†	NO	YES	NO
115-7	DISK TO BAR (d)	YES	YES	YES
115-8	DISK TO BAR (d)	YES	YES	YES
115-9	DISK TO BAR (c)	NO	NO	NO
115-10	DISK TO BAR (c)	NO	YES	NO
115-11	DISK TO BAR (e)§	YES	NO	NO
115-12	DISK TO BAR (e)§	YES	NO	NO
115-13	DISK TO BAR (e)	YES	YES	YES
115-14	DISK TO BAR (d)	NO	YES	NO
115-15	DISK TO BAR (d)	NO	YES	NO
115-16	DISK TO BAR (e)	YES	YES	YES

* High voltage (HV) electrode to low voltage (LV) electrode arrangement used for each experiment. The letter in parentheses indicates the particular electrode arrangement shown in Figure 2-2.

† In sample 115-6 a 5 mil copper foil was used in lieu of the brass bar. This was found to cause excessive electrical noise pick-up on the PVDF pressure sensor.

TABLE A-3. PVDF PRESSURE SENSOR DATA

SAMPLE NUMBER	$\Delta t_{bk\text{-}P1}$ (μs)	$\Delta t_{P1\text{-}P2}$ (μs)	$P_{1\ peak}$ (nC)	$P_{2\ peak}$ (nC)
115-2	4.8	4.3	137	106
115-3	4.8	3.6	112	106
115-8	20.0	5.4	-	87
115-9	17.6	5.6	-	156
115-10	10.2	6.0	627	152
115-11	1.8	8.8	128	91
115-13*	4.2	-	94	-
115-15*	3.2	-	134	-
115-16*	3.0	-	117	-
ALW-1	4.0	7.74	>50	>50
ALW-2	3.3	4.2	196	>77
NRT-1	2.0	19.2	374	43
NRT-2	14.1	12.2	173	113
NRT-3†	3.1	19.4	>700	67
NRT-4§	33.7	6.3	117	48
AIR-7	21.1	-	102	-
AIR-8	-	"	-	18

* Experiments 115-13 through 115-16 used a 1/4" thick PMMA backing plate behind the bottom end cap. The second PVDF sensor was not used.

† The confinement ring was not used for experiment NRT-3.

§ The second pressure sensor was not supported by any backing plate in experiment NRT-4.

" The time delay between breakdown and the second PVDF signal in experiment AIR-8 was 53.8 μs.

Key:
ALW - aluminized wax samples.
NRT - inert samples from MICOM.
AIR - air gap experiments.
$\Delta t_{bk\text{-}P1}$ - Delay between breakdown and the first PVDF signal.
$\Delta t_{P1\text{-}P2}$ - Delay between first and second PVDF signal.

DISTRIBUTION

	Copies
Chief of Naval Research	
Attn: ONR 1132P (R. Miller)	1
ONT 20T (L. V. Schmidt)	1
ONT 213 (D. Siegel)	1
ONT 23 (A. J. Faulstich)	1
ONT 232 (D. Hauser)	1
800 N. Quincy Street, BCT 1	
Arlington, VA 22217-5000	
OUSDRE/R&AT-MST	
Attn: R. Siewart	1
The Pentagon	
Washington, DC 20301	
OUSDRE/TWP-NW&M	
Attn: D. Anderson	1
The Pentagon	
Washington, DC 20301	
OUSDRE/TWP--OM	
Attn: G. Kopcsak	1
The Pentagon	
Washington, DC 20301	
USD(A)/DDRE (R/AT/ET)	
Staff Specialist for Weapons Technology	
Attn: F. Menz	1
The Pentagon	
Washington, DC 20301	
OASN/RE&S	
Attn: Surface Warfare	1
Air Warfare	1
Subs/ASW	1
Navy Department	
Washington, DC 20301	

	Copies
Chairman	
Department of Defense Explosives Safety Board	
Attn: 6-A-145	1
DDESB-KT	1
Hoffman Building 1	
2461 Eisenhower Avenue	
Alexandria, VA 22331	
Chief of Naval Operations	
Attn: OP-098	1
OP-981	1
OP-982	1
OP-983	1
OP-987	1
OP-02T	1
OP-22	1
OP-225	1
OP-32	1
OP-35	1
OP-37	1
OP-374	1
OP-501	1
OP-502	1
OP-503	1
OP-72	1
OP-74	1
OP-75	1
Navy Department	
Washington, DC 20350	
Commander	
Space and Naval Warfare Systems Command	
Attn: SPAWAR-05	1
Washington, DC 20363-5100	

DISTRIBUTION (Cont.)

		Copies
Commander		
Naval Sea Systems Command		
Attn:	SEA-05R	1
	SEA-55	1
	SEA-55X	1
	SEA-55X1	1
	SEA-55X2	1
	SEA-55Y	1
	SEA-66U	1
	SEA-62	1
	SEA-62Y	1
	SEA-62Z	1
	SEA-63	1
	SEA-63D	1
	PMS-402	1
	PMS-406	1
	PMS-407	1
Washington, DC 20362-5105		
Commander		
Naval Air Systems Command		
Attn:	AIR-5004	1
	AIR-51623	1
	AIR-540	1
	AIR-5404	1
	AIR-93	1
	AIR-932F	1
	AIR-932H	1
	AIR-932K	1
	AIR-932T	1
	PMA-242	1
	Technical Library	1
Washington, DC 20361		
Commander		
David Taylor Research Center		
Attn:	Technical Library	1
	Code 17	1
	Code 172	1
	Code 1740.3 (R. Garrison)	1
	Code 1740.4 (S. Wang)	1
	Code 175 (W. Sykes)	1
	Code 1750.2 (W. Conley)	1
	Code 1740.2 (F. Fisch)	1
Bethesda, MD 20084		

		Copies
Commander		
David Taylor Research Center		
Attn:	Code 177	1
	Technical Library	1
Portsmouth, VA 20375		
Commanding Officer		
Naval Research Laboratory		
Attn:	Technical Library	1
Washington, DC 20375		
Commanding Officer		
Naval Coastal Systems Center		
Attn:	Technical Library	1
Panama City, FL 32407-5000		
Commander		
Naval Underwater Systems Center		
Attn:	Technical Library	1
Newport, RI 02840		
Commander		
Naval Weapons Center		
Attn:	Code 3917	1
	Code 38 (R. Derr)	1
	Code 389 (T. Boggs)	1
	Code 32	1
	Code 3205	1
	Code 3208	1
	Code 326	1
	Code 326B (G. Greene)	1
	Code 326B (L. Josephson)	1
	Code 3261	1
	Code 3263	1
	Code 3264	1
	Code 3265	1
	Code 3266	1
	Code 327	1
	Code 381	1
	Code 385	1
	Code 3850	1
	Code 3853	1
	Code 3891 (J.Covino)	1
	Code 39	1
	Technical Library	1
China Lake, CA 93555		

DISTRIBUTION (Cont.)

	Copies
Commanding Officer Naval Ordnance Station	
Attn: Code 2730D	1
Technical Library	1
J. Chang	1
P. Dendor	1
L. Newman	1
Indian Head, MD 20640-5000	
Commander Center for Naval Analyses	
Attn: Technical Library	1
2000 Suitland Road Washington, DC 20390-5140	
Superintendent Naval Postgraduate School	
Attn: Library	1
Monterey, CA 93940	
President Naval War College	
Attn: Technical Library	1
Newport, RI 02841	
Commanding Officer Naval Amphibious Base, Coronado	
Attn: RDT Officer	1
SEAL Team	1
Underwater Demolition Team	1
San Diego, CA 92155	
Commanding Officer Naval Amphibious Base Little Creek	
Attn: RDT Officer	1
Norfolk, VA 23511	
Commanding Officer Naval Explosive Ordnance Disposal Technology Center	
Attn: Technical Library	1
Indian Head, MD 20640	

	Copies
Commander Pacific Missile Test Center	
Attn: Code 2145	1
Point Mugu, CA 93042	
Commanding Officer SEAL Team 2	
FPO New York, NY 09501-4633	1
Commanding Officer Naval Undersea Warfare Engineering Station	1
Keyport, WA 98345	
Commanding Officer Naval Ship Weapons Systems Engineering Station	1
Port Hueneme, CA 93043	
Commander Naval Weapons Evaluation Facility	
Kirtland Air Force Base Albuquerque, NM 87117	1
Commanding Officer Naval Weapons Support Center	
Attn: Code 3031 (E. Neal)	1
Code 50D (A. Norris)	1
Code 505 (J. E. Short)	1
Code 90 (A. E. Whitner)	1
Crane, IN 47522	
Commanding Officer Naval Weapons Station	
Attn: Code 321 (M. Bucher)	1
Concord, CA 94520-5000	
Commanding Officer Naval Weapons Station	
Attn: Code 470A	1
Library	1
Yorktown, VA 23691-5000	
Director Defense Nuclear Agency	
Attn: Technical Library	1
Washington, DC 20305	

DISTRIBUTION (Cont.)

	Copies
Defense Science Board Attn: C. Fowler The Pentagon Washington, DC 20301	1
Director Defense Research and Engineering Attn: Library Washington, DC 20305	1
Director Defense Advanced Research Projects Agency Attn: Library 1400 Wilson Blvd. ARlington, VA 22209	1
Institute for Defense Analyses Attn: Technical Library 1801 N. Beauregard Street Alexandria, VA 22311	1
Commanding General Marine Corps Development and Education Command Attn: Library Marine Corps Landing Force Development Center Quantico, VA 22134	1
Army Armament Munitions and Chemical Command Attn: DRSAR-IRC DRSAR-LEM (R. Freeman) DRSAR-SF (R. Young) Rock Island, IL 61299-6000	1 1 1
Army Armament Research and Development Command Attn: Technical Library Dover, NJ 07801	1
Redstone Arsenal Army Missile Command Attn: Chief, Documents D. Dreitzler Redstone Arsenal, AL 35809	1 1
Army Ballistic Research Laboratory Attn: SLC-BR-TB-EE SLCRBR-IB-I (P. Kaste) V. Boyle O. Blake G. Melani M. Chawla J. Trimble Technical Library Aberdeen Proving Ground Aberdeen, MD 21005-5066	1 1 1 1 1 1 1 1
Commander Officer Harry Diamond Laboratory Attn: Library 2800 Powder Mill Road Adelphi, MD 20783	1
Army Environmental Hygiene Agency Attn: HSHB-EA-A Aberdeen Proving Ground Aberdeen, MD 21005	1
Army Medical Bioengineering Research and Development Laboratory Attn: J. Barkeley Fort Dietrick, MD 21701	1
Commander Army Research Office Attn: G. R. Husk P. O. Box 12211 Research Triangle Park, NC 27709-2211	1
Army Toxic and Hazardous Materials Agency Attn: DRXTH-TE-D Aberdeen Proving Ground Aberdeen, MD 21005	1
Commander Army Chemical Research, Development and Engineering Center Attn: SMCCR-DDP Aberdeen Proving Ground, MD 21010-5423	1

DISTRIBUTION (Cont.)

	Copies
Air Force Armament Division	
Attn: AFATL/MNE	1
AFATL/MNW	1
AFATL/DLODL	1
Library	1
Eglin Air Force Base, FL 32542-6009	
Air Force Office of Scientific Research	
Attn: T. Matusko	1
Bolling Air Force Base	
Washington, DC 20332	
University of California	
Lawrence Livermore National Laboratory	
Attn: Technical Library	1
M. Finger	1
C. M. Tarver	1
J. D. Hallquist	1
L. M. Erickson	1
E. James	1
P. O. Box 808	
Livermore, CA 94550	
Los Alamos National Laboratory	
Attn: J. Repa	1
M. J. Urizar	1
S. W. Peterson	1
L. Smith	1
C. Forest	1
A. W. Campbell	1
R. Engelke	1
P. C. Crawford	1
Los Alamos, NM 87545	
Sandia National Laboratories	
Attn: Technical Library	1
P. O. Box 969	
Livermore, CA 94550-0096	
Argonne National Laboratory	
Attention Records Control for:	
Richard Anderson	1
Technical Library	1
9700 South Cass Avenue	
Argonne, IL 60439	

	Copies
The Johns Hopkins University	
Applied Physics Laboratory	
Chemical Propulsion Information Agency	
Attn: T. W. Christian	1
Johns Hopkins Road	
Laurel, MD 20707	
The Johns Hopkins University	
Applied Physics Laboratory	
Attn: Technical Library	1
Johns Hopkins Road	
Laurel, MD 20707	
New Mexico Institute of Mining Technology	
Attn: Code TERA (J. Joyner)	1
Technical Library	1
Socorro, NM 87801	
Applied Research Laboratory	
Pennsylvania State University	
Attn: Library	1
E. Liska	1
P. O. Box 30	
University Park	
State College, PA 16801	
Defense Technical Information Center	
Cameron Station	
Alexandria, VA 22304-6142	12
Royal Armament Research and Development Establishment	
Attn: B. Hammant	1
Fort Halstead	
Sevenoaks, Kent, United Kingdom	
Advanced Technology and Research, Inc.	
Attn: S. Jacobs	1
J. W. Watt	1
W. Pickler	1
Laurel Technology Center	
14900 Sweitzer Lane	
Laurel, MD 20707	

DISTRIBUTION (Cont.)

	Copies
TRW	
Attn: R. Church	1
San Bernadino, CA 92401	
Aerojet Ordnance and Manufacturing Company	
Attn: G. Chin	1
9236 East Hall Road	
Downey, CA 90241	
Vanderbilt University	
Attn: A. Mellor	1
Nashville, TN 37235	
Lockheed Missiles and Space Company	
Attn: R. Hodges	1
J. Smith	1
P. O. Box 504	
Sunnyvale, CA 94086	
Hercules Incorporated Rocket Center	
Attn: G. Williams	1
P. O. Box 210	
Rocket Center, WV 26726	
Hercules	
Attn: M. Klakken	1
M. Berger	1
L. Losee	1
T. Speed	1
Bacchus Works	
Magna, UT 84044-0098	
Internal distribution:	
E231	2
E232	3
G13 (D. L. Dickinson)	1
G13 (T. Wasmond)	1
G22 (W. H. Holt)	1
(W. Mock)	1
(S. S. Waggener)	1
R10	1
R101 (R. Doherty)	1

		Copies
Internal distribution (Cont.)		
R10	(R. R. Bernecker)	1
	(C. Dickinson)	1
	(H. S. Haiss)	1
	(L. A. Roslund)	1
R11		1
R12		1
R12	(B. A. Baudler)	1
	(T. D. Chung)	1
	(L. C. Hudson)	1
	(G. Laib)	1
	(L. L. Mensi)	1
	(L. J. Montesi)	1
	(P. F. Spahn)	1
R13		1
R13	(J. W. Forbes)	5
	(R. D. Bardo)	1
	(C. S. Coffey)	1
	(J. Davis)	1
	(D. L. Demske)	1
	(B. C. Glancy)	1
	(R. H. Guirguis)	1
	(P. K. Gustavson)	1
	(H. D. Jones)	1
	(K. Kim)	1
	(R. J. Lee)	1
	(W. W. Lee)	1
	(E. R. Lemar)	1
	(T. P. Liddiard)	1
	(P. J. Miller)	1
	(C. T. Richmond)	1
	(H. W. Sandusky)	1
	(G. T. Sutherland)	1
	(D. G. Tasker)	1
	(W. H. Wilson)	1
	(D. L. Woody)	1
	(F. J. Zerilli)	1
R14		1
R14	(J. W. Koenig)	1
R15		1
R42	(R. Dewitt)	1
U10	(W. Wassmann)	1
U11	(R.Plenge)	1
	(D. Hinely)	1
U32	(G. Parrent)	1

REPORT DOCUMENTATION PAGE

Form Approved
OMB No. 0704-0188

1. AGENCY USE ONLY *(Leave blank)*	2. REPORT DATE	3. REPORT TYPE AND DATES COVERED
	December 1991	Final Report

4. TITLE AND SUBTITLE
Electrostatic Discharge Initiation Experiments using PVDF Pressure Transducers

5. FUNDING NUMBERS
Program Element No.
Project No.
Task No.
Work Unit No.

6. AUTHOR(S)
R. J. Lee, D. G. Tasker, and M -T. Cong

7. PERFORMING ORGANIZATION NAME(S) AND ADDRESS(ES)
Naval Surface Warfare Center
10901 New Hampshire Avenue
Silver Spring, MD 20903-5000

8. PERFORMING ORGANIZATION REPORT NUMBER
NAVSWC TR 91-666

9. SPONSORING/MONITORING AGENCY NAME(S) AND ADDRESS(ES)
Office of Naval Technology
800 N. Quincy Street
Arlington, VA 22217-5000

10. SPONSORING/MONITORING AGENCY REPORT NUMBER

11. SUPPLEMENTARY NOTES

12a. DISTRIBUTION/AVAILABILITY STATEMENT
Approved for public release; distribution is unlimited.

12b. DISTRIBUTION CODE

13. ABSTRACT *(Maximum 200 words)*

Electrical discharge experiments were performed on an aluminized explosive, PBXW-115. Simultaneous observations of polyvinylidene difluoride (PVDF) pressure sensor signals, and the deposition of electrical power were recorded. These data were compared to those from similar experiments performed on aluminized inert material and in air gaps. Distinct pressure differentials were observed during the discharge phase following a delay after dielectric breakdown. The signals from the pressure sensors are comparable for each case, i.e., the unreacted PBXW-115, the ignited PBXW-115, the inert solids, and the air gaps. It is believed that sustained ignition occurred in the explosive after the electrical energy deposition following a long incubation period (< 10 ms). Containment of the building reaction, and the presence of air adjacent to the explosive sample, were found to have a significant effect on the ignition sensitivity. The results are discussed within the context of a preliminary model of electrostatic initiation.

14. SUBJECT TERMS

Electrostatic Discharge	Dielectric Breakdown
Ignition	Arc Discharge
PBXW-115	PVDF Pressure Gauge

15. NUMBER OF PAGES
39

16. PRICE CODE

17. SECURITY CLASSIFICATION OF REPORT	18. SECURITY CLASSIFICATION OF THIS PAGE	19. SECURITY CLASSIFICATION OF ABSTRACT	20. LIMITATION OF ABSTRACT
UNCLASSIFIED	UNCLASSIFIED	UNCLASSIFIED	SAR